A ROBUST SCHEME FOR THE MULTICOMPONENT REACTIVE GAS FLOWS IN THE PRESENCE OF SHOCK WAVES

Z.M. Hu,[1] R.S. Myong*[2] and T.H. Cho[2]

충격파가 존재하는 혼합 반응기체 유동장 해석을 위한 수치기법

Z.M. Hu,[1] 명 노 신,*[2] 조 태 환[2]

In this paper, the dispersion controlled dissipative (DCD) scheme is reviewed and then extended to simulate chemically reacting gas flows in multicomponent mixtures in the presence of strong shock waves. Furthermore, the properties of the reactive DCD (DCD-R) scheme are discussed, followed by several applications. The DCD scheme has been shown to have the following features: high accuracy and robustness for reacting gas flows in the presence of strong shock waves and contact discontinuities, and algorithmic simplicity.

Key words : multicomponent, reacting flow, shock capturing, robust scheme

1. INTRODUCTION

Chemically reacting gas flows are of interest across a wide scope of research or engineering applications, such as combustion, space shuttle reentry, propulsion, and chemical laser problems. A great deal of numerical effort has been made to illustrate the underlying physical and chemical phenomenon in the relevant flows. However, the simulation of chemically reacting flow presents distinct difficulties associated with the inherently large ranges of spatial and temporal scales involved, and the stiffness of the governing differential equations. It becomes even more difficult to satisfy the corresponding numerical requirements in the presence of strong shock waves and contact discontinuities. On the other hand, most of the prevailing schemes for shock capturing, either flux difference splitting (FDS) or flux vector splitting (FVS), were initially developed for inert flows. When a scheme is extended to multicomponent reacting flows, the complex formula manipulation becomes inevitable. Moreover, the robustness of the consequential scheme may suffer from the stiffness introduced by chemical reactions.

The dispersion controlled dissipative (DCD) scheme, which was proposed by Jiang[1-3], is one of the shock capturing schemes to deal with the stiffness problem. The principle of the DCD scheme is to suppress nonphysical oscillation by making use of the inherent dispersion characteristics of the modified equation rather than by adding artificial viscosity. In complex flowfields there may be many shock waves or discontinuities with a large scope of intensities. The artificial dissipation required must vary in accordance with the oscillation amplitude that depends on the discontinuity intensity so that optimum effects could be achieved. Unfortunately, it is too difficult to be realized; therefore, over or under-dissipation may be introduced into numerical solutions. Moreover, the free parameters for controlling artificial dissipation have no physical meaning and may induce something artificial. The DCD scheme has been demonstrated to be distinct from conventional dissipation-based schemes in which special attention was not given to the problem of the nonphysical

접수일: 2007년 2월 15일, 심사완료일: 2007년 3월 21일.

1 경상대학교 항공기부품기술연구소

2 종신회원, 경상대학교 기계항공공학부 및 항공기부품기술연구소

* Corresponding author, E-mail: myong@gnu.ac.kr

oscillation that occurs in the vicinities of shock waves or contact discontinuities. This scheme has sufficient dissipation to remove the carbuncle phenomenon, which is a numerical instability when capturing a strong shock wave in multidimensional computations. The DCD scheme has the following features: accuracy and robustness for shock and contact discontinuities, algorithmic simplicity, and computational efficiency for multicomponent reacting flows[4].

In this paper, the DCD scheme is first reviewed and then the scheme formulation for multicomponent systems is demonstrated, which is referred to as DCD-R scheme for briefness in the following text. Furthermore, the properties of the DCD-R scheme are discussed, followed by several applications.

2. DISPERSION-CONTROLLED DISSIPATIVE SCHEMES FOR THE MULTICOMPONENT REACTIVE FLOWS

2.1 REVIEW OF THE DCD SCHEME FOR SHOCK CAPTURING

In the sample wave equation

$$\frac{\partial u}{\partial t}+c\frac{\partial u}{\partial x}=0,\quad c>0, \tag{1}$$

the partial differential equation (1) must be discretized on the discretized numerical domain to obtain a finite difference equation at grid point j:

$$u_j^{t+\Delta t}=f\left(u_{j+l}^t\right),\quad l=\pm 1,\cdots,\pm L. \tag{2}$$

Here parameter L varies according to the numerical scheme used for discretization. When all of the terms in (2) are extended with the Taylor series at grid point j, a new partial differential equation can be derived in the form of

$$\frac{\partial u}{\partial t}+c\frac{\partial u}{\partial x}=\sum_{i=2}^{\infty}\mu_i\frac{\partial^i u}{\partial x^i}. \tag{3}$$

Eq. (3) was referred to as the modified equation of the finite difference equation by Warming and Hyett in 1974[5]. The numerical solution of the finite difference equation (2) is essentially the solution of the modified equation (3) rather than (1). From the viewpoint of the modified equation, the nonphysical oscillations and the smeared shock waves are not induced by numerical errors or by perturbations possibly introduced in the computational procedure, but instead represent the intrinsic characteristics of the modified equation (3). Starting from the analysis of the modified equation of the simple wave equation (1), Jiang brought forward the dispersion condition for non-oscillatory shock capturing schemes[1-3]. A single term in the series of the exact solution can be given as

$$u_m(x,t)=\exp(C_1t)\cdot\exp(ik[x-(c+C_2)t]), \tag{4}$$

where

$$C_1=\sum_{n=1}^{\infty}(-1)^n k_m^{2n}\mu_{2n}$$
$$\text{and } C_2=\sum_{n=1}^{\infty}(-1)^{n+1}k_m^{2n}\mu_{2n+1}. \tag{4.1}$$

Here, the first term on the right side represents the wave amplitude evolution resulting from all of the dissipation terms in the modified equation. The second term denotes the wave propagating speed that depends on all of the dispersion terms. Warming and Hyett[5] defined the stability condition, $C_1<0$. However, artificial viscosity should be added to suppress the oscillation near the shock waves. In Jiang's shock capturing scheme[1,2], artificial viscosity is no longer necessary when the dispersion conditions are determined as $C_2>0$ behind shock waves, and $C_2<0$ in front of shock waves. The primary idea underlying these conditions is to force high-frequency waves to concentrate at a shock wave by actively changing the sign of the phase shift errors of numerical schemes across a shock wave. The dispersion conditions, together with the Warming's stability condition, are considered to be sufficient conditions for any non-oscillatory shock capturing scheme[1,2].

For the one-dimensional (1D) Euler equation

$$\frac{\partial U}{\partial t}+\frac{\partial F(U)}{\partial x}=0, \tag{5}$$

Jiang formed the second order DCD (dispersion controlled dissipative) scheme as

$$\left(\frac{\partial U}{\partial t}\right)_j=-\frac{1}{\Delta x}(H_{j+1/2}^n-H_{j-1/2}^n), \tag{6}$$

with

$$H^n_{j+1/2} = F^+_{j+1/2L} + F^-_{j+1/2R}, \tag{6.1}$$

$$F^+_{j+1/2L} = F^+_j + 0.5\Phi^+_A \cdot \min\mathrm{mod}\left(\Delta F^+_{j-1/2}, \Delta F^+_{j+1/2}\right), \tag{6.2}$$

$$F^-_{j+1/2R} = F^-_{j+1} - 0.5\Phi^-_A \cdot \min\mathrm{mod}\left(\Delta F^-_{j+1/2}, \Delta F^-_{j+3/2}\right), \tag{6.3}$$

$$\Delta F^\pm_{j+1/2} = F^\pm_{j+1} - F^\pm_j, \tag{6.4}$$

$$F^\pm = A^\pm U, \tag{6.5}$$

$$\Phi^\pm_A = I \mp \beta\Lambda^\pm_A, \text{ and} \tag{6.6}$$

$$\min\mathrm{mod}(a,b) = \begin{cases} 0, & ab \le 0 \\ sign(a) \cdot \min(abs(a), abs(b)), & else \end{cases} \tag{6.7}$$

where I is a unit matrix, $\beta = \Delta t/\Delta x$, and Λ_A is the diagonal matrix consisting of the eigenvalues of the Jacobian matrix $A = \partial F(U)/\partial U$. In these formulas, the minmod limiter acts automatically as a shock wave identifier, and flux vector splitting at a midpoint is carried out using the Steger and Warming method[6].

2.2 Extension to the Multicomponent Reactive Flows

2.2.1 Governing Equations

This section extends the DCD scheme to the DCD-R scheme for reactive flows in premixed multicomponent mixtures. For simplification, only the unsteady convective and reacting equations in two dimensional (2D) Cartesian coordinates are considered as the governing equations,

$$\frac{\partial U}{\partial t} + \frac{\partial F}{\partial x} + \frac{\partial G}{\partial y} = S. \tag{7}$$

Here, the vector consisting of unknown variables, U, the convective flux vectors, F and G, and the chemical reaction source term, S are written as

$$U = \begin{bmatrix} \rho C_1 \\ \rho C_2 \\ \vdots \\ \rho C_{ns} \\ m \\ n \\ E \end{bmatrix}, F = \begin{bmatrix} mC_1 \\ mC_2 \\ \vdots \\ mC_{ns} \\ m^2/\rho + p \\ mn/\rho \\ (E+p)m/\rho \end{bmatrix}, G = \begin{bmatrix} nC_1 \\ nC_2 \\ \vdots \\ nC_{ns} \\ mn/\rho \\ n^2/\rho + p \\ (E+p)n/\rho \end{bmatrix}, S = \begin{bmatrix} \dot{\omega}_1 \\ \dot{\omega}_2 \\ \vdots \\ \omega_{ns} \\ 0 \\ 0 \\ 0 \end{bmatrix}. \tag{7.1}$$

These are the common forms and there are also other asymmetric forms in some literature. Compared to the governing system (5) for a pure gas fluid, the current system includes a continuity equation and the production term for each component. Here, the total density of the mixture and partial density of the species i are denoted by ρ and ρ_i, and $c_i = \rho_i/\rho (i = 1, ns)$ is mass fraction of the corresponding species. $m = \rho u$ and $n = \rho v$ are momentums in the x and y directions, respectively. The total energy density E is defined as

$$E = \rho h - p + \rho(u^2 + v^2)/2. \tag{7.2}$$

Each species is usually assumed to be a thermally perfect gas, and the specific heat and enthalpy for each species can be calculated by the thermal polynomial equations given in[7]:

$$\frac{h_i}{R_i T} = -a_{1i}T^{-2} + a_{2i}T^{-1}\ln T + a_{3i} + \frac{a_{4i}}{2}T + \frac{a_{5i}}{3}T^2 + \frac{a_{6i}}{4}T^3 + \frac{a_{7i}}{5}T^4 - \frac{a_{8i}}{2}T^{-3} + \frac{a_{9i}}{T} \tag{7.3.1}$$

Therefore, the mixture enthalpy h is the summation of all the partial component enthalpies in the mixture, as follows:

$$h = \sum_{i=1}^{n_s} c_i h_i. \tag{7.3.2}$$

According to Dalton's law, the pressure p is the sum of the partial pressures of all species. It can be calculated by the state equation:

$$p = \sum_{i=1}^{n_s} \rho_i R_i T, \tag{7.4}$$

where, R_i is the gas constant of species i, and T is the temperature of the gas mixture. For an elementary chemical reaction, the chemical production rate $\dot{\omega}_i$, derived from a reaction mechanism of nr chemical reactions, can be calculated by

$$\dot{\omega}_i = W_i \sum_{r=1}^{NR} (\nu'_{ir} - \nu''_{ir}) \left(k_{fr} \prod_{j=1}^{n_s} (\chi_j)^{\nu'_{ir}} - k_{br} \prod_{j=1}^{n_s} (\chi_j)^{\nu''_{ir}} \right), \tag{7.5}$$

where i and j denote the species number in the r th elementary reaction. The molecular weight of each species is denoted by W_i. ν'_{ir} and ν''_{ir} are the stoichiometric coefficient of species i in the r th reaction that appear as the reactant and product, respectively. The molecular concentration of each species is denoted by χ_j. k_{fr} and

k_{br} denote the forward and the backward reaction rates. The forward reaction rate of each reaction is calculated by the Arrhenius law (Eq. 7.5.1) and the corresponding backward reaction rate can be derived from the equilibrium constant (Eq. 7.5.2 - 7.5.3) and k_{fr}.

$$k_{fr} = C_r T^{mr} \exp[-Ea_r/RT], \tag{7.5.1}$$

$$\kappa_{br} = \kappa_{fr}/\kappa_{er}, \tag{7.5.2}$$

$$\kappa_{er} = \exp\left(\sum_{i=1}^{ns}\left[(\nu''_{ir}-\nu'_{ir})\left(\frac{s_{ir}}{R_{ir}}-\frac{h_{ir}}{R_{ir}T}\right)\right]\right) \cdot \left(\frac{P_{atm}}{RT}\right)^{\sum_{i=1}^{ns}(\nu''_{ir}-\nu'_{ir})}. \tag{7.5.3}$$

More thermodynamic properties of each species, such as the specific heat at a constant pressure and the specific entropy, are given in[7], as follows:

$$Cp_i/R_i = a_{1i}T^{-2}+a_{2i}T^{-1}+a_{3i}+a_{4i}T + a_{5i}T^2+a_{6i}T^3+a_{7i}T^4+a_{8i}T^{-3} \tag{7.6.1}$$

$$\frac{S_i}{R_i} = -\frac{a_{1i}}{2}T^{-2}-a_{2i}T^{-1}+a_{3i}\ln T+a_{4i}T + \frac{a_{5i}}{2}T^2+\frac{a_{6i}}{3}T^3+\frac{a_{7i}}{4}T^4+\frac{a_{8i}}{3}T^{-3}+a_{10} \tag{7.6.2}$$

2.2.2 DCD-R SCHEMES

During the computation, the contribution from the fluid dynamic terms is calculated first to obtain an intermediate value of $\widetilde{U}'$. This is followed by a calculation accounting for the chemical reaction contribution to evaluate $\widetilde{U}$ for the next time step. This approach, termed the operator-split algorithm as shown in (8), allows separate calculations of the fluid dynamic and chemical reaction contributions with different time steps to satisfy the Δt consistent with the CFL condition and the required time scale for the stiff ODEs of the reactions, respectively.

$$L(\Delta t) = L_{conv}\left(\frac{\Delta t}{2}\right)\left[\sum_{n=1}^{N} L_{chem}\left(\frac{\Delta t}{N}\right)\right] L_{conv}\left(\frac{\Delta t}{2}\right) \tag{8}$$

The convective operator in (8) is implemented with the DCD scheme. This is described in the following section. The Jacobian matrices for the multicomponent system are $A=\partial F/\partial U$, $B=\partial G/\partial U$. For simplification and symmetry, the first one is given here as:

$$A = \begin{bmatrix} (1-C_1)u & -C_1u & \cdots & -C_1u & C_1 & 0 & 0 \\ -C_2u & (1-C_2)u & \cdots & -C_2u & C_2 & 0 & 0 \\ \vdots & \vdots & \ddots & \vdots & \vdots & \vdots & \vdots \\ -C_{ns}u & -C_{ns}u & \cdots & (1-C_{ns})u & C_{ns} & 0 & 0 \\ p_{\rho_1}-u^2 & p_{\rho_2}-u^2 & \cdots & p_{\rho_{ns}}-u^2 & p_m+2u & p_n & p_E \\ -uv & -uv & \cdots & -uv & v & u & 0 \\ (p_{\rho_1}-H)u & (p_{\rho_2}-H)u & \cdots & (p_{\rho_{ns}}-H)u & H+up_m & up_n & (1+p_E)u \end{bmatrix}. \tag{9}$$

Here,

$$p_E = \sum_{i=1}^{ns} C_iR_i \Big/ \left(\sum_{i=1}^{ns} C_iCp_i - \sum_{i=1}^{ns} C_iR_i\right) = \frac{\hat{R}}{\hat{Cp}-\hat{R}} = \frac{\hat{Cp}}{\hat{Cp}-\hat{R}} - 1 = \hat{\gamma}-1 \tag{9.1}$$

$$p_{\rho_i} = (1+p_E)R_iT - p_E\left(h_i - \frac{u^2+v^2}{2}\right), \tag{9.2}$$

$$p_m = -up_E, \quad p_n = -vp_E, \text{ and} \tag{9.3}$$

$$H = (E+p)/\rho. \tag{9.4}$$

The eigenvalues of the matrix A are obtained as:

$$\{\lambda_1, \lambda_2, \cdots \lambda_{ns+1}, \lambda_{ns+2}, \lambda_{ns+3}\} = \{u, u, \cdots u, u-a, u+a\}, \tag{10}$$

where $a = \sqrt{(H-u^2-v^2)p_E + \sum_{i=1}^{ns} C_ip_{\rho_i}} = \sqrt{\hat{\gamma}\hat{R}T}$ is the frozen sound speed of the mixture. In the above equations, the circumflex over a variable represents the corresponding property of the mixture. Therefore, the diagonal matrix containing the eigenvalues is

$$\Lambda = diag\{\lambda_1, \lambda_2, \cdots, \lambda_{ns}, \lambda_{ns+1}, \lambda_{ns+2}, \lambda_{ns+3}\}. \tag{11}$$

At the same time, the corresponding left and right eigenvectors of the Jacobian matrix A are denoted by L and R, where $L=R^{-1}$ and $A=R\cdot\Lambda\cdot L$. With the formulas mentioned above, two flux-splitting methods for the DCD-R scheme are illustrated and discussed.

Based on the eigenvalue splitting, the first flux vector splitting uses the Steger-Warming (SW) method[6],

$$\lambda_s^{\pm} = \frac{1}{2}(\lambda_s \pm |\lambda_s+\varepsilon|), \; s=1,\cdots ns+3, \; 0<\varepsilon \ll 1. \tag{12}$$

The split fluxes can be obtained directly by

$$F^{\pm}=A^{\pm}U=(R\cdot\Lambda^{\pm}\cdot L)\cdot U$$
$$=\frac{\rho}{2\hat{\gamma}}\begin{bmatrix} C_1[2(\hat{\gamma}-1)\lambda_1^{\pm}+\lambda_{ns+2}^{\pm}+\lambda_{ns+3}^{\pm}] \\ C_2[2(\hat{\gamma}-1)\lambda_1^{\pm}+\lambda_{ns+2}^{\pm}+\lambda_{ns+3}^{\pm}] \\ \vdots \\ C_{ns}[2(\hat{\gamma}-1)\lambda_1^{\pm}+\lambda_{ns+2}^{\pm}+\lambda_{ns+3}^{\pm}] \\ u[2(\hat{\gamma}-1)\lambda_1^{\pm}]+(u-a)\lambda_{ns+2}^{\pm}+(u+a)\lambda_{ns+3}^{\pm} \\ v[2(\hat{\gamma}-1)\lambda_2^{\pm}+\lambda_{ns+2}^{\pm}+\lambda_{ns+3}^{\pm} \\ 2[(\hat{\gamma}-1)H-a^2]\lambda_1^{\pm}+(H-au)\lambda_{ns+2}^{\pm}+(H+au)\lambda_{ns+3}^{\pm} \end{bmatrix}. \quad (13)$$

Therefore, with the split fluxes given by (13), the DCD-R scheme is ready for a multicomponent system that has a similar form and formulary process to those described in (6). The split form of G is symmetric to that of F.

The second method is the Lax-Friedrichs (LF) flux splitting

$$F^{\pm}=R\cdot[L\cdot(F\pm\alpha U)]$$
$$=\frac{\rho}{2}\begin{bmatrix} C_1(u\pm\alpha) \\ C_2(u\pm\alpha) \\ \vdots \\ C_{ns}(u\pm\alpha) \\ u(u\pm\alpha)+\dfrac{p}{\rho} \\ v(u\pm\alpha) \\ \rho H(u\pm\alpha)\mp\alpha\dfrac{p}{\rho} \end{bmatrix} \quad (14)$$

where $\alpha=\max_{1\le s\le ns+3}(\lambda_s)$. The flux form appears even simpler than the SW splitting.

With the SW (13) or LF (14) split flux mentioned above, it is possible to implement the DCD scheme given in (6) to obtain the numerical flux. The formulation is straightforward and the matrix operation can be avoided in programming. An alternative computational procedure is a characteristic-wise flux splitting. In this method, the DCD scheme is handled with the split flux in the characteristic space in order to obtain an intermediate flux, which is further projected back into the physical space to obtain the final numerical flux. First, the variables shall be transformed into the local characteristic space using

$$W=L\cdot U. \quad (15)$$

Second, the SW or LF flux splitting operation is applied to each component of the flux in the characteristic space by

$$\widetilde{F^{\pm}}(W)=\Lambda^{\pm}\cdot W \quad \text{or} \quad (16)$$

$$\widetilde{F^{\pm}}(W)=\frac{1}{2}[L\cdot F(U)\pm\alpha W]. \quad (17)$$

With these split fluxes, the DCD scheme is performed to obtain the numerical flux in the characteristic fields, as mentioned in (6),

$$\widetilde{H}=\widetilde{F^{+}}+\widetilde{F^{-}}. \quad (18)$$

Finally, the numerical flux is transformed back into the physical space using

$$H=R\cdot\widetilde{H}. \quad (19)$$

In this method, the matrix operation and characteristic decomposition are needed in computation. Hence, the computational cost is greatly increased, but the method is much more robust.

2.3 Properties of the DCD-R Scheme

For the testing of the scheme properties, a shock tube problem in a mixture of air is given, which is approximated by $4N_2+O_2$. The set-up is a Riemann-type initial condition

$$U(x,0)=\begin{cases} U_L, & 0\le x\le 0.5 \\ U_R, & 0.5\le x\le 1 \end{cases}, \quad (20)$$

with $p_L=24160Pa$, $T_L=375K$, $p_R=2416Pa$, $T_R=300K$. The normalized density, pressure and the Mach number are shown in Figs. 1 and 2. In Fig. 1, it is clear that the DCD-R scheme implemented with SW flux splitting (13), performs well when the second-order Runge-Kutta method and CFL $\le$ 0.75 are used for the time marching. However, the nonphysical oscillation at a low frequency results from the discontinuity contact when CFL = 0.6 and the first-order time integration is used, and severe oscillation at a high frequency occurs near the leading shock when CFL = 1 and the second-order Runge-Kutta method is used.

As shown in Fig. 2(a), the LF splitting (15, 17-19) solution appears nearly identical to SW splitting (13), except that a slight discrepancy is present near the rarefaction wave tail or the discontinuity contact. However, the CFL constraint is less rigorous if the LF splitting algorithm is applied in the characteristic space, as in Fig. 2(b). Even with a high CFL number of 1, a smooth solution can be obtained without any nonphysical oscillation. Numerical experiments show that the SW

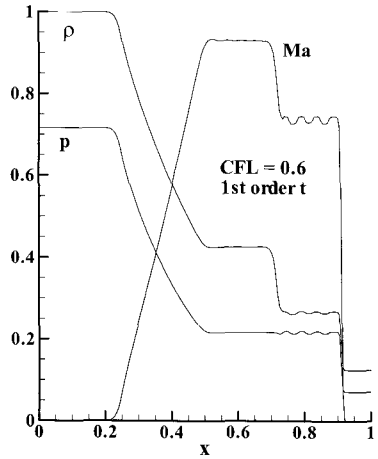

(a) CFL=0.6 and time order=1,

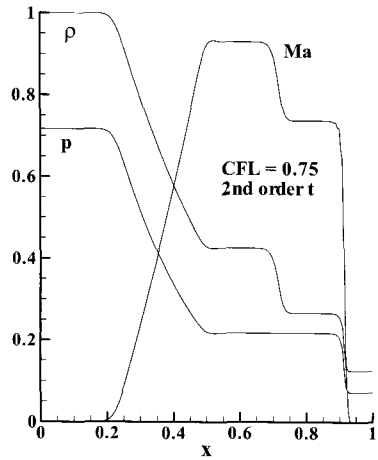

(b) CFL=0.75 and time order=2,

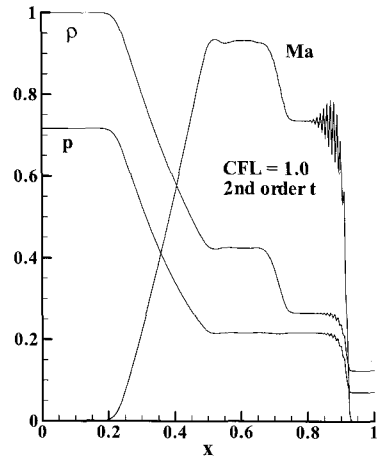

(c) CFL=1.0 and time order=2

Figure 1 DCD-R solutions (SW splitting) to the shock tube problem in a multicomponent mixture (grid node: 200).

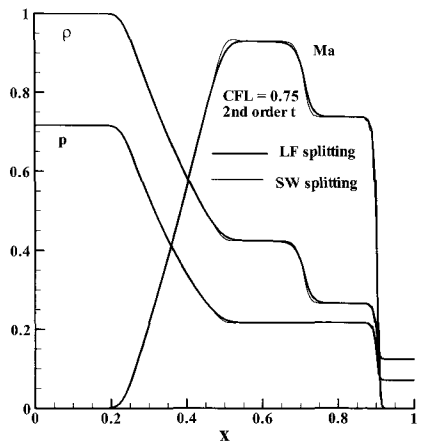

(a) CFL=0.75, flux splitting in physical space,

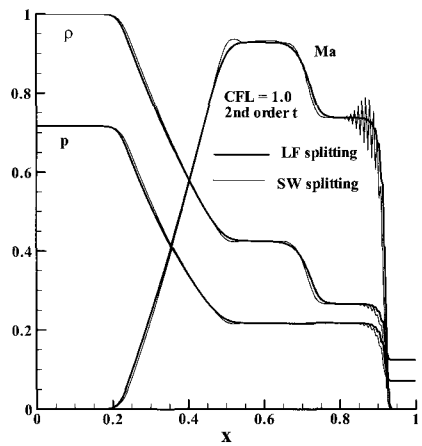

(b) CFL=1.0, LF flux splitting in characteristic space

Figure 2 Comparison of the SW and LF flux splitting methods (grid node: 200).

splitting method with the characteristic decomposition (15,16,18,19) has the familiar performance of the LF splitting (15, 17-19).

Due to the algorithmic simplicity and computational efficiency, the SW (13) or LF (14) splitting method without a matrix operation is recommended for the DCD-R scheme. In addition, it is not possible to use a high CFL number for chemically reactive flow simulations as the required time marching step is primarily determined by the stiff reaction terms. This can also explain the use of the simple SW flux splitting in[1,2].

2.4 VERIFICATION

To verify the numerical algorithms for multicomponent reacting flows, detonation waves reflections from wedges

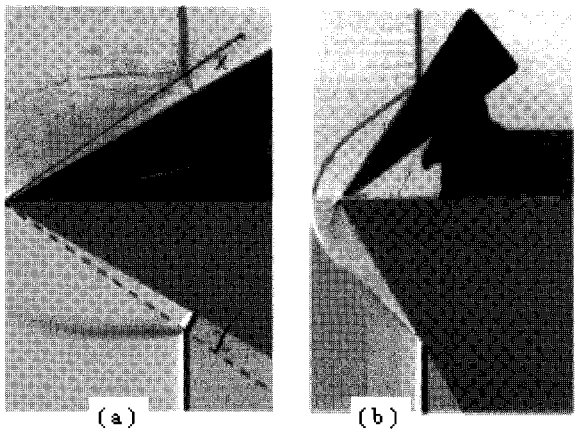

Figure 3 Verification by a comparison of the numerical (lower half) and experimental Schlieren[8] (upper half) results of the detonation reflections over wedges with angles of (a) 30°, and (b) 60° in a mixture of $2H_2+O_2+Ar$, P_0=20 kPa.

with different wedge angles in stoichiometric mixtures of hydrogen and oxygen diluted by 25% Argon ($2H_2+O_2+Ar$, P_0=20kPa at room temperature) were simulated and then compared with experimental Schlieren results. Two types of reflection mechanisms of detonation waves, regular and Mach reflections are shown in Fig. 3, in which the experimental pictures are placed in the upper half and the numerical results in the lower half. From these figures, it can be seen that the angle of the triple point trajectory, χ in Fig. 3(a) and the reflection angle in Fig. 3(b) are in good agreement with the experiments.

3. APPLICATIONS

3.1 CASE 1: SHOCK TUBE PROBLEM

In a ground test facility, such as a shock tunnel, the primary objective is to generate high enthalpy flows to simulate the actual flight conditions around a high-speed vehicle. In the first application case, the shock tube problem is utilized again to demonstrate that a lighter driver gas with a smaller molecular weight can achieve a test flow with higher total enthalpy. The initial set-up is as follows: the pressure ratio, $p_2/p_1 = 10000$, the temperature ratio, $T_2/T_1 = 1.25$, the test gas is $4N_2+O_2$, and two types of driver gases, $4N_2+O_2$ and He, are used. The results are shown in Fig. 4. The total enthalpy of the test gas with the helium driver gas increases three-fold compared to that with the air driver gas.

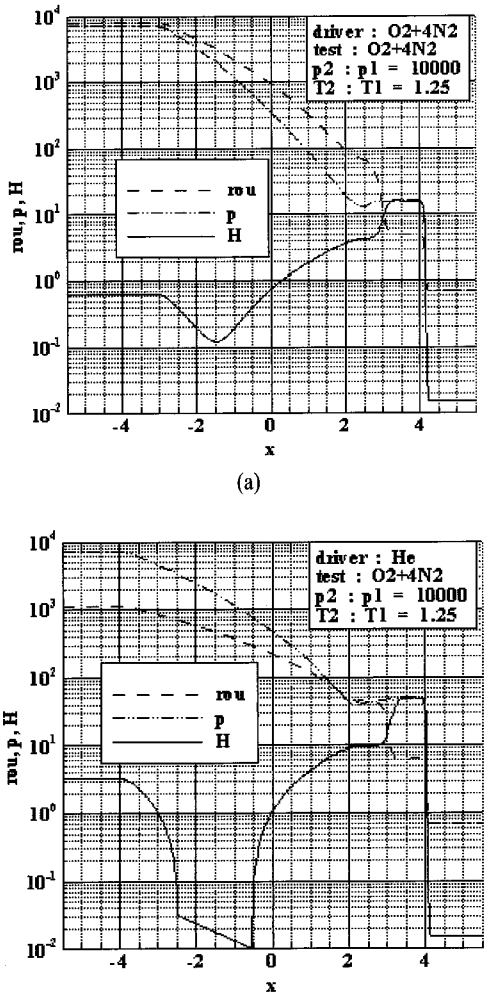

Figure 4 Shock tube problem for high-enthalpy test flows.

3.2 CASE 2: DETONATION WAVE PROPAGATION

In short, a detonation wave is a strong shock wave followed by a reaction zone. The energy released from the reaction zone supports the leading shock, while the adiabatic compression of the leading shock facilitates the induction or exothermic reaction. These kinetic and gas dynamic processes allow a detonation wave coupling and further allow it to be self-sustaining. It is well known that in the detonation front structure, the leading shock is wrinkled and consists of alternating weak incident shocks and stronger Mach stems that are jointed at triple points by transverse waves that travel back and forth perpendicular to the wave front and extend back into the

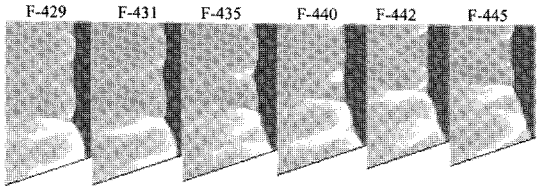

Figure 5 Multi-wave front structure of a detonation wave diffracting over a wedge surface.

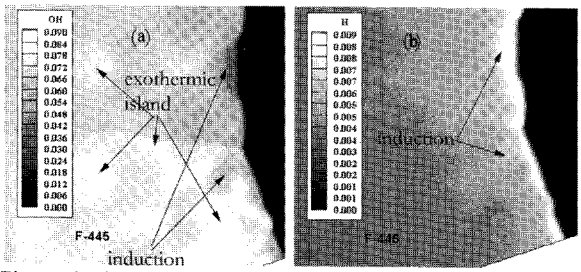

Figure 6 The reactive components and the asymmetri reaction fields.

reaction zones. The transverse waves interact with the reaction zones behind the leading shock and induce endothermic induction or an exothermic combination that depends on the local wave structures. From the viewpoint of mathematics, the problem of detonation wave propagation can be simplified as an unsteady, convective, and reacting flow.

The DCD-R scheme was applied to simulate the detonation diffraction over wedge surfaces as reported in[4]. Several results are given in Figs. 5 and 6. In particular, Fig. 5 shows the evolution of the multi-wave structures, collisions between transverse waves, and the alternating of the incident shocks and Mach stems while a cellular detonation wave is diffracting. Figure 6 illustrates the distribution of the reactive components and the asymmetrical reaction fields induced by the complicated wave processes mentioned above.

4. CONCLUSIONS

In this paper, the principle of the dispersion controlled dissipative (DCD) scheme is briefly reviewed and then extended to simulate chemically reacting flows in multicomponent mixtures in the presence of strong shock waves. In addition, the property of the reactive DCD (DCD-R) scheme is discussed by investigating shock tube problems with different driver gases and wave dynamic processes as a cellular detonation wave diffracts over a wedge surface. The DCD scheme was shown to have favorable features such as high accuracy and robustness for chemically reacting flows in the presence of strong shock waves and algorithmic simplicity.

ACKNOWLEDGEMENTS

This work was supported by Korea Research Foundation (Grant No. KRF-2005-005-J09901) and the second stage Brain Korea 21 project.

REFERENCES

[1] Jiang, Z.L., Takayama, K. and Chen, Y.S., 1995, "Dispersion conditions for non-oscillatory shock capturing schemes and its applications," *Computational Fluid Dynamics Journal*, Vol.4, pp.137-150.

[2] Jiang, Z.L., 2003, "Reliable validation based on optical flow visualization for CFD simulation," *ACTA Mechanica Sinica*, Vol.19, No.3, pp.193-203.

[3] Jiang, Z.L., 2005, "On dispersion-controlled principles for non-oscillatory shock-capturing schemes," *ACTA Mechanica Sinica*, Vol.20, No.1, pp.1-15.

[4] Hu, Z.M., Gao, Y.L., Zhang, D.L., Yang, G.W. and Jiang, Z.L., 2004, "Numerical simulation of gaseous detonation reflection over wedges with a detailed chemical reaction model (in Chinese)," *ACTA Mechanica Sinica*, Vol.36, No.4, pp.385-391.

[5] Warming, R.F. and Hyett, B.J., 1974, "The modified equation approach to the stability and accuracy analysis of finite difference equation methods," *Journal of Computational Physics*, Vol.14, pp.159-179.

[6] Steger, J.L. and Warming, R.F., 1981, "Flux vector splitting of the inviscid gas-dynamic equations with application to finite difference methods," *Journal of Computational Physics*, Vol.40, pp.263-293.

[7] Mcbride, B.J., Zehe, M.J., and Gordon, S., 2002, "NASA Glenn coefficients for calculating thermodynamic properties of individual species," *NASA/TP* 2002-211556.

[8] Thomas, G.O. and Williams, R.L., 2002, "Detonation interaction with wedges and bends," *Shock Waves*, Vol.11, pp.481-492.